

## Physical and Functional Interactions of Human DNA Polymerase $\eta$ with PCNA

LAJOS HARACSKA,<sup>1</sup> ROBERT E. JOHNSON,<sup>1</sup> ILDIKO UNK,<sup>1</sup> BARBARA PHILLIPS,<sup>2</sup>  
JERARD HURWITZ,<sup>2</sup> LOUISE PRAKASH,<sup>1</sup> AND SATYA PRAKASH<sup>1\*</sup>

*Sealy Center for Molecular Science, University of Texas Medical Branch, Galveston, Texas 77555-1061,<sup>1</sup>  
and Department of Molecular Biology and Virology, Memorial Sloan-Kettering  
Cancer Center, New York, New York 10021-6007<sup>2</sup>*

Received 5 July 2001/Returned for modification 20 July 2001/Accepted 27 July 2001

**Human DNA polymerase  $\eta$  (hPol $\eta$ ) functions in the error-free replication of UV-damaged DNA, and mutations in hPol $\eta$  cause cancer-prone syndrome, the variant form of xeroderma pigmentosum. However, in spite of its key role in promoting replication through a variety of distorting DNA lesions, the manner by which hPol $\eta$  is targeted to the replication machinery stalled at a lesion site remains unknown. Here, we provide evidence for the physical interaction of hPol $\eta$  with proliferating cell nuclear antigen (PCNA) and show that mutations in the PCNA binding motif of hPol $\eta$  inactivate this interaction. PCNA, together with replication factor C and replication protein A, stimulates the DNA synthetic activity of hPol $\eta$ , and steady-state kinetic studies indicate that this stimulation accrues from an increase in the efficiency of nucleotide insertion resulting from a reduction in the apparent  $K_m$  for the incoming nucleotide.**

DNA polymerase  $\eta$  (Pol $\eta$ ) is unique among eukaryotic DNA polymerases in its proficient ability to replicate through distorting DNA lesions. Both in yeast and in humans, Pol $\eta$  functions in the error-free replication of UV-damaged DNA (19, 26, 34, 39), and mutations in human Pol $\eta$  (hPol $\eta$ ) result in cancer-prone syndrome, the variant form of xeroderma pigmentosum (XP-V) (17, 25). Interestingly, both yeast Pol $\eta$  and hPol $\eta$  replicate through a *cis-syn* thymine-thymine (TT) dimer with the same efficiency and accuracy as they replicate through undamaged T's (18, 21, 37). Also, genetic studies with yeast have indicated a role for Pol $\eta$  in the error-free bypass of cyclobutane pyrimidine dimers that are formed at 5'-TC-3' and 5'-CC-3' sites (40). Pol $\eta$  also promotes replication through a (6-4) TT photoproduct, a highly distorting DNA lesion, by preferentially inserting a G residue opposite the 3' T of the photoproduct. Subsequently, Pol $\zeta$  efficiently promotes extension from the G residue by inserting the correct nucleotide, A, opposite the 5' T of the lesion (16). Although the insertion of a G opposite the 3' T of the (6-4) TT photoproduct would cause 3' T→C substitutions, it was previously suggested that a similar insertion of G by Pol $\eta$  opposite the 3' C of the 5'-TC-3' and 5'-CC-3' (6-4) photoproducts, followed by extension by Pol $\zeta$  by the insertion of the correct nucleotide opposite the 5' residue of this lesion, would lead to error-free bypass of the DNA lesion (16). Since (6-4) photoproducts are formed much more frequently at TC and CC sites than at TT sites (4, 6), Pol $\eta$  would largely contribute to the error-free bypass of (6-4) lesions as well. Yeast Pol $\eta$  and hPol $\eta$  also efficiently replicate through other DNA lesions, such as 8-oxoguanine (15) and O<sup>6</sup>-methylguanine (13).

The ability of Pol $\eta$  to replicate through distorting DNA lesions has suggested that the active site of Pol $\eta$  is tolerant of geometric distortions introduced into DNA by these lesions. As a consequence, Pol $\eta$  is a low-fidelity enzyme, and on undamaged DNA, the yeast and human enzymes misincorporate nucleotides with a frequency of 10<sup>-2</sup> to 10<sup>-3</sup> (21, 38). In sharp contrast, replicative DNA polymerases exhibit a much higher fidelity, misinserting nucleotides with a frequency of 10<sup>-4</sup> to 10<sup>-7</sup> (3, 8, 33). However, because of their enhanced sensitivity to geometric distortions in DNA (9), these polymerases are unable to replicate through DNA lesions.

Although hPol $\eta$  plays a critical role in the error-free replication of UV-damaged DNA and thus prevents the formation of sunlight-induced skin cancers, the manner by which this polymerase gains access to the replication machinery stalled at a lesion site is not known. Here, we examine the role of proliferating cell nuclear antigen (PCNA) in promoting the access of hPol $\eta$  to the replication machinery. PCNA, a ring-shaped homotrimeric protein, forms a sliding clamp at the primer-template junction. PCNA is loaded onto DNA by the multi-protein clamp loader, replication factor C (RFC), which couples ATP hydrolysis to open and close the PCNA ring around the DNA. Replication protein A (RPA) binds single-stranded DNA, and after the loading of PCNA, RFC stays on DNA via its interaction with RPA (2, 22, 41). The replicative DNA polymerase, Pol $\delta$ , then assembles with the PCNA ring, and this association endows the polymerase with a high processivity (30, 32). However, because of its inability to replicate through DNA lesions such as cyclobutane pyrimidine dimers, Pol $\delta$  stalls at such lesion sites (18), necessitating the action of a translesion synthesis polymerase, such as Pol $\eta$ . Here, we provide evidence for the physical interaction of hPol $\eta$  with PCNA and show that PCNA, together with RFC and RPA, stimulates the DNA synthetic activity of hPol $\eta$ . These studies identify PCNA as a crucial element for the assembly of hPol $\eta$  into the replication machinery.

\* Corresponding author. Mailing address: Sealy Center for Molecular Science, University of Texas Medical Branch, 6.104 Blocker Medical Research Building, 11th and Mechanic Streets, Galveston, TX 77555-1061. Phone: (409) 747-8602. Fax: (409) 747-8608. E-mail: sprakash@scms.utmb.edu.

## MATERIALS AND METHODS

**Proteins.** Human PCNA (hPCNA), RFC, and RPA were purified as described previously (5, 10, 24). Six-His-tagged hPCNA, used for interaction studies, was overexpressed in *Escherichia coli* and purified as described previously (23). Wild-type and mutant hPol $\eta$  proteins fused with glutathione S-transferase (GST) were purified as described previously (16, 21); for the DNA synthesis studies (see Fig. 3 and 4), the GST portion was removed by treatment with PreScission protease (Amersham Pharmacia Biotech).

**Generation of *hRAD30A* mutations.** To generate the *hRAD30A*  $F^{707}$ - $F^{708}$   $\rightarrow$   $A^{707}$ - $A^{708}$  and the *hRAD30A* (1-695) mutations, a portion of the 3' end of the *hRAD30A* gene was amplified by PCR using oligonucleotide N4919 (5'-GGGG TGTCGA AGCTAGAAG AATCCTCTA AAGCAACTCC-3' (17) and mutagenic oligonucleotides N7819 (5'-CCTGGGATCC TAATGTGTTA ATGGCT TAG CAGCTGATTC CAATGTTTG CATGCC-3') and N7820 (5'-CTTGG GATCC TAGCGTTTAT TAGTGCAGGC CAAAGGGCTC-3'), respectively. The *hRAD30A* (1-695) mutant gene encodes only amino acid residues 1 to 695. A 223-bp *Asp*718/*Bam*HI PCR fragment containing the *hRAD30A*  $F^{707}$ - $F^{708}$   $\rightarrow$   $A^{707}$ - $A^{708}$  mutation and a 169-bp *Asp*718/*Bam*HI PCR fragment containing the *hRAD30A* (1-695) mutation were cloned into plasmid YIplac211, generating plasmids pBJ835 and pBJ840, respectively. The cloned PCR fragments in pBJ835 and pBJ840 were sequenced to confirm the presence of the mutations. Subsequently, an *Asp*718 DNA fragment containing the rest of the *hRAD30A* gene was cloned into plasmids pBJ835 and pBJ840; the *hRAD30A* open reading frame was restored, but either the *hRAD30A*  $A^{707}$ - $A^{708}$  or the *hRAD30A* (1-695) mutation was retained. Each *hRAD30A* mutant gene was cloned in frame with the GST gene under the control of the galactose-inducible phosphoglycerate kinase promoter in pBJ842, generating plasmids pBJ867 and pBJ868, respectively. For the yeast two-hybrid analysis, the *hRAD30A* (1-695) and *hRAD30A*  $A^{707}$ - $A^{708}$  mutant genes and the wild-type *hRAD30A* gene were cloned in frame with the GAL4 DNA binding domain (BD) (amino acid residues 1 to 147) in plasmid pAS1, and the resulting plasmids were designated pR30.219, pR30.220, and pR30.218, respectively. Also, for these studies, hPCNA was cloned in frame with the GAL4 activation domain (AD) in plasmid pPCNA1.32.

**DNA polymerase assays.** The circular DNA substrate used for some of the DNA synthesis studies (see Fig. 3A) was a 7.2-kb M13mp18 single-stranded DNA primed with a nonlabeled 36-nucleotide oligomer spanning nucleotides 6330 to 6294. For the processivity assays shown in Fig. 3B and the kinetic studies shown in Fig. 4, we used a single-stranded M13-derived (M13mp7L2) DNA primed with a 5'  $^{32}$ P-labeled oligomer primer, LP-097, 5'-GGGTAACGCCAG GGTTCCTCCAGTCACGACGTTGTAAAACGACGGCCAG-3'. The standard DNA polymerase reaction mixture (10  $\mu$ l) contained 40 mM Tris-HCl (pH 7.5); 8 mM MgCl<sub>2</sub>; 150 mM NaCl; 1 mM dithiothreitol; 100  $\mu$ g of bovine serum albumin/ml; 500  $\mu$ M ATP; and 100  $\mu$ M each dGTP, dATP, dTTP, and dCTP. For reactions with a circular DNA substrate primed with a nonlabeled oligonucleotide (see Fig. 3A),  $\alpha$ - $^{32}$ P-labeled dATP (final dATP concentration,  $\sim$ 200 to 500 cpm/pmol) was added. When needed, wild-type or mutant hPol $\eta$  (10 ng), PCNA (100 ng), RFC (50 ng), and/or RPA (250 ng) was incubated with 25 ng of M13 DNA substrate. Assays were assembled on ice and incubated at 37°C for 10 min, and the reaction was stopped by the addition of loading buffer (40  $\mu$ l) containing EDTA (20 mM), 95% formamide, 0.3% bromophenol blue, and 0.3% cyanol blue. The reaction products were resolved on 10% polyacrylamide gels containing 8 M urea. Quantitation of the results was done using a Molecular Dynamics STORM PhosphorImager and ImageQuant software.

**Processivity assays.** hPol $\eta$  (10 ng) was preincubated with a circular M13 primer-template DNA substrate (50 ng) in standard reaction buffer, which contained no deoxynucleotides, for 5 min at 37°C. Reactions were initiated by adding all four deoxynucleoside triphosphates (dNTPs) (500  $\mu$ M each) or all four dNTPs plus excess sonicated herring sperm DNA (0.5 mg/ml) as a trap. To demonstrate the effectiveness of the trap, hPol $\eta$  was preincubated with the DNA trap and the primer-template substrate before the addition of dNTPs.

**Steady-state kinetic analyses.** Steady-state kinetic analyses for deoxynucleotide incorporation opposite an A or a C site were performed as described previously (7, 11). Briefly, hPol $\eta$  alone or in the presence of PCNA, RFC, and RPA was incubated with increasing concentrations of a single dNTP for 10 min under standard reaction conditions. In the running-start assay, each reaction included dTTP (15  $\mu$ M). Gel band intensities of the substrates and products were quantitated with a PhosphorImager, and the percentage of primer extension was plotted as a function of dNTP concentration. The data were fit by nonlinear regression, using SigmaPlot 5.0, to the Michaelis-Menten equation describing a hyperbola,  $v = (V_{\max} \times [dNTP]) / (K_m + [dNTP])$ . Apparent  $K_m$  and  $V_{\max}$  steady-state parameters were obtained from the fit and used to calculate the efficiency of deoxynucleotide incorporation ( $V_{\max}/K_m$ ).

**Physical interaction of hPol $\eta$  with PCNA.** To make complexes, wild-type or mutant GST-hPol $\eta$  proteins (4  $\mu$ g) were mixed with six-His-hPCNA (4  $\mu$ g) in 75  $\mu$ l of buffer I [50 mM Tris-HCl (pH 7.5), 150 mM NaCl, 1 mM Tris(2-carboxyethyl)-phosphine-HCl, 0.01% Nonidet P-40, 10% glycerol] and incubated for 30 min at 4°C followed by 10 min at 25°C. Subsequently, to 25  $\mu$ l of these samples, either 10  $\mu$ l of glutathione-Sepharose (Pharmacia) beads or 10  $\mu$ l of Ni-nitrilotriacetic acid (NTA) (Qiagen) beads was added to bind GST-Pol $\eta$  or six-His-PCNA and their complexes, respectively. The samples were further incubated with rocking for 30 min at 4°C. The glutathione-Sepharose and Ni-NTA beads were washed five times each with buffer I, followed by elution of the bound proteins with buffer I containing 40 mM glutathione and 500 mM imidazole, respectively. All protein samples, including the protein mixture before the addition of affinity beads, the flowthrough plus wash fractions, and the eluted proteins, were precipitated with 5% trichloroacetic acid (TCA) and separated on a sodium dodecyl sulfate-12% polyacrylamide gel followed by Coomassie blue R-250 staining.

**Two-hybrid analyses.** The HF7c yeast cell line was transformed with the GAL4 BD-hPol $\eta$  and the GAL4 AD-hPCNA fusion constructs. Transformants harboring both the GAL4 BD-hPol $\eta$  and the GAL4 AD-hPCNA fusion constructs were grown on synthetic complete media lacking leucine and tryptophan.  $\beta$ -Galactosidase activity was examined to determine the interaction between hPol $\eta$  and PCNA as described in the Clontech Yeast Protocols Handbook (PT3024-1; chapter VI). Experiments were performed at least three times with triplicate samples.

## RESULTS

Generating mutations in the PCNA binding motif of hPol $\eta$ .

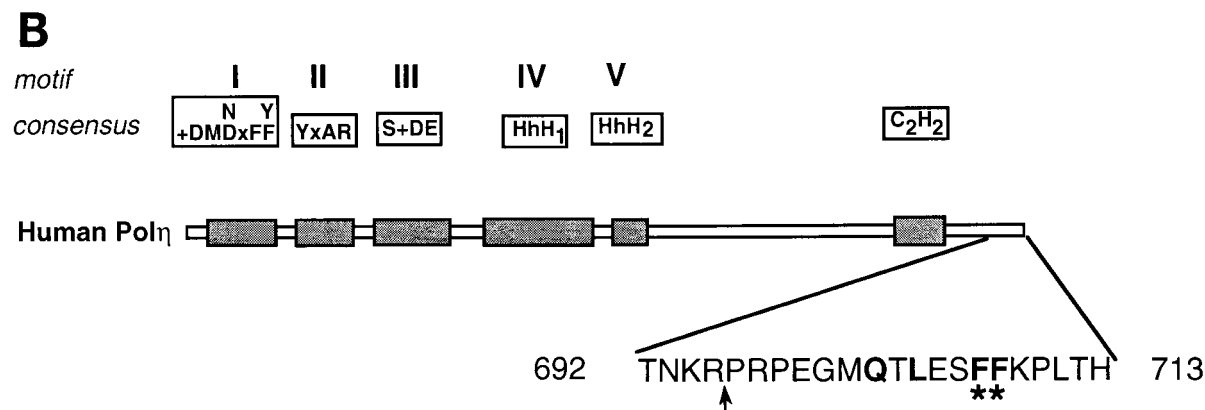
Many proteins involved in DNA replication and repair contain a consensus PCNA binding motif, QXX(I, L, or M)XXF(F or Y) (22, 35), and structural and mutational studies have indicated the involvement of the conserved hydrophobic residues within this motif in the interaction with PCNA (27, 31, 36). In the protein sequence of hPol $\eta$ , the product of the human *RAD30A* gene, a putative PCNA binding sequence, Q-TLESFF, is located at the extreme C terminus and encompasses residues 702 to 708 of the 713-amino-acid protein (Fig. 1). To test if this motif was involved in the interaction of hPol $\eta$  with PCNA, two mutations in the *hRAD30A* gene were generated, *rad30A* (1-695) and *rad30A*  $A^{707}$ - $A^{708}$ . In the hPol $\eta$  (1-695) protein, the C-terminal 18 amino acids, including the conserved F<sup>707</sup> and F<sup>708</sup> residues of the putative PCNA binding motif (Fig. 1B), have been removed, whereas in the hPol $\eta$   $A^{707}$ - $A^{708}$  protein, both of these phenylalanine residues have been changed to alanines (Fig. 1B). The wild-type and mutant hPol $\eta$  proteins were expressed in yeast as GST fusion proteins. During purification, the mutant hPol $\eta$  proteins displayed the same chromatographic properties as the wild-type protein, and the proteins were at least 95% pure, as judged from Coomassie blue staining (data not shown). To rule out the possibility that the mutations caused improper folding, the DNA polymerase activities of the wild-type and mutant hPol $\eta$  proteins were compared. Running start-DNA synthesis reactions were carried out using a linear DNA substrate either containing or not containing a *cis-syn* TT dimer. The wild-type and mutant hPol $\eta$  (1-695) and hPol $\eta$   $A^{707}$ - $A^{708}$  proteins displayed identical DNA polymerase and TT dimer bypass activities (data not shown).

**Interaction of hPol $\eta$  with PCNA—two-hybrid analysis.** We used the yeast two-hybrid system to examine the interaction of hPol $\eta$  and hPCNA proteins *in vivo*. In one of the plasmids, the GAL4 BD was fused with either wild-type *RAD30A* or mutant *rad30* (1-695) or *rad30*  $A^{707}$ - $A^{708}$  open reading frames, and in the other plasmid, the GAL4 AD was fused with hPCNA. The HF7c yeast reporter strain harboring the GAL4 AD-hPCNA

**A**

Hs p21	K R R <b>Q</b> T S <b>M</b> T D <b>F</b> Y H S K R
Hs Fen1	G S T <b>Q</b> G R L D D <b>F</b> F K V T G
Hs MSH3	P A R <b>Q</b> A V L S R <b>F</b> F Q S T G
Sc Rad27	S G I <b>Q</b> G R L D G <b>F</b> F Q V V P
Hs XP-G	Q Q T <b>Q</b> L R I D S <b>F</b> F R L A Q
Sc Rad2	K G K <b>Q</b> K R I N E <b>F</b> F P R E Y
Sc Cdc9	K P K <b>Q</b> A T L A R <b>F</b> F T S M K
Sc MSH6	K M K <b>Q</b> S S L L S <b>F</b> F S K Q V
Sc Pol32	L K K <b>Q</b> G T L E S <b>F</b> F K R K A
Sc Rad30	V T S <b>S</b> K N I L S <b>F</b> F T R K K
Hs Rad30A	E G M <b>Q</b> - T L E S <b>F</b> F K P L T
Consensus	<b>Q</b> - - <b>L</b> - - <b>F</b> <b>F</b> I M

**FIG. 1.** PCNA binding motif of hPol $\eta$ . (A) C-terminal amino acids 699 to 712 of hPol $\eta$  are aligned with the PCNA binding motifs identified in various PCNA binding proteins. The highly conserved residues are shown in bold. Hs, human; Sc, *S. cerevisiae*. (B) Mutations made in the PCNA binding motif of hPol $\eta$ . In the schematic representation of hPol $\eta$ , the five highly conserved motifs (I to V) shared among different members of the Pol $\eta$ /UmuC/DinB protein family are indicated, and the C<sub>2</sub>H<sub>2</sub> motif conserved in the Pol $\eta$  family is shown (20). The amino acid residues present in the extreme C-terminal region are shown; the amino acids highly conserved in the consensus PCNA binding motif are shown in bold. In the hPol $\eta$  (1-695) mutant protein, the last 18 amino acids from the C terminus were deleted (indicated by an arrow). In the hPol $\eta$  A<sup>707</sup>-A<sup>708</sup> mutant protein, the F residues at positions 707 and 708 (indicated by asterisks) were changed to A residues.



plasmid was transformed with one of the GAL4 BD-hPol $\eta$  plasmids. The expression of GAL4 BD-hPol $\eta$  fusion proteins was confirmed by immunoblotting using anti-hPol $\eta$  antibodies (data not shown). The interaction of the wild-type and mutant hPol $\eta$  proteins with PCNA in these transformants was analyzed by a  $\beta$ -galactosidase liquid assay, and the results are summarized in Table 1. Compared to the low level of  $\beta$ -galactosidase activity detected with the wild-type GAL4 BD-hPol $\eta$  protein and the GAL4 AD protein, the wild-type GAL4 BD-hPol $\eta$  protein showed a strong interaction with PCNA bound to GAL4 AD, resulting in 21-fold higher level of  $\beta$ -galactosidase activity. Deletion or point mutations in the conserved PCNA binding site in the hPol $\eta$  (1-695) and hPol $\eta$  A<sup>707</sup>-A<sup>708</sup> proteins strongly reduced the interaction between hPol $\eta$  and PCNA, yielding only a small increase in  $\beta$ -galactosidase activity. These results establish an interaction of hPol $\eta$  with PCNA in vivo and show that the PCNA binding motif at the C terminus of hPol $\eta$  plays an important role in mediating this interaction.

**Physical interaction of hPol $\eta$  with PCNA.** Next, we examined if purified hPol $\eta$  physically interacts with purified hPCNA in vitro. Wild-type GST-hPol $\eta$  or mutant GST-hPol $\eta$  (1-695) or GST-hPol $\eta$  A<sup>707</sup>-A<sup>708</sup> proteins were incubated with six-His-PCNA, and a pull down assay was carried out using Ni-NTA or glutathione-Sepharose affinity beads (Fig. 2). As expected, the Ni-NTA beads bound only six-His-PCNA and not GST-hPol $\eta$  (Fig. 2, lanes 10 to 12) and the glutathione-Sepharose beads bound GST-hPol $\eta$  but not six-His-PCNA (Fig. 2, lanes 22 to 24). Hence, the two proteins could be pulled down together only if they interacted with one another.

When six-His-PCNA was bound to the Ni-NTA beads, a large proportion of wild-type hPol $\eta$  remained bound to PCNA

(Fig. 2, lanes 1 to 3); similarly, when GST-hPol $\eta$  was bound to the glutathione-Sepharose beads, PCNA was retained on the beads via an interaction with hPol $\eta$  (Fig. 2, lanes 13 to 15). However, the interaction of hPol $\eta$  with PCNA was greatly reduced for both the hPol $\eta$  A<sup>707</sup>-A<sup>708</sup> and the hPol $\eta$  (1-695) mutant proteins. For example, when six-His-PCNA was bound to the Ni-NTA beads, almost all of each mutant hPol $\eta$  protein was recovered in the flowthrough (Fig. 2, lanes 5 and 8); conversely, when the mutant hPol $\eta$  proteins were bound to the glutathione-Sepharose beads, the majority of PCNA was recovered in the flowthrough (Fig. 2, lanes 17 and 20). Thus, hPol $\eta$  interacts with PCNA in vitro, and mutations in the conserved PCNA binding motif of hPol $\eta$  reduce this interaction very substantially.

**PCNA cooperates with RFC and RPA to enhance the DNA synthetic activity of hPol $\eta$ .** Next, we examined if PCNA stimulates the DNA synthetic activity of hPol $\eta$ . Stimulation of the synthetic activity of the replicative DNA polymerase, Pol $\delta$ , by PCNA requires the action of RFC and RPA as well. Therefore, we examined the effect of PCNA on the DNA synthetic activity

**TABLE 1.** Interaction of hPol $\eta$  with hPCNA in the yeast two-hybrid system

BD fusion <sup>a</sup>	AD fusion	Mean $\pm$ SD $\beta$ -galactosidase activity	Fold activation
GAL4 BD-hPol $\eta$ (WT)	GAL4 AD	0.82 $\pm$ 0.05	1
GAL4 BD-hPol $\eta$ (WT)	GAL4 AD-hPCNA	17.6 $\pm$ 0.6	21
GAL4 BD-hPol $\eta$ A <sup>707</sup> -A <sup>708</sup>	GAL4 AD-hPCNA	1.75 $\pm$ 0.03	2
GAL4 BD-hPol $\eta$ (1-695)	GAL4 AD-hPCNA	2.71 $\pm$ 0.05	3

<sup>a</sup> WT, wild type.

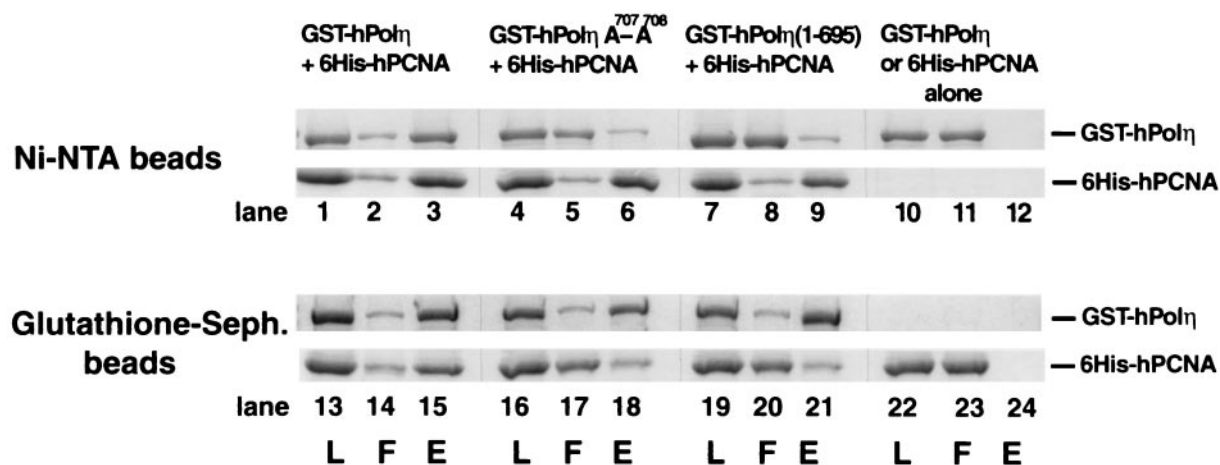


FIG. 2. Pol $\eta$  forms a complex with PCNA. Six-His-hPCNA (4  $\mu$ g) was mixed either with wild-type GST-hPol $\eta$  protein (lanes 1 to 3 and 13 to 15) or with mutant GST-hPol $\eta$  A<sup>707-708</sup> (lanes 4 to 6 and 16 to 18) or GST-hPol $\eta$  (1-695) (lanes 7 to 9 and 19 to 21) protein (4  $\mu$ g each). As controls, the same amounts of GST-hPol $\eta$  (lanes 10 to 12) or six-His-hPCNA (lanes 22 to 24) protein were used alone. After incubation, samples were bound to Ni-NTA (lanes 1 to 12) or glutathione-Sepharose (Seph.) (lanes 13 to 24) beads, followed by washing and elution of the bound proteins by imidazole- or glutathione-containing buffer, respectively. Aliquots of each sample before loading on the beads (L), the flowthrough and wash (F), and the eluted proteins (E) were precipitated by TCA and analyzed on a sodium dodecyl sulfate-12% polyacrylamide gel stained with Coomassie blue. The positions of GST-hPol $\eta$  and six-His-hPCNA are indicated on the right.

of hPol $\eta$  in the presence of RFC and RPA by using a single-stranded M13 template DNA primed at a unique site (Fig. 3A). The DNA synthetic activity of hPol $\eta$  is enhanced ~12-fold upon the addition of PCNA, RFC, and RPA (Fig. 3A, compare lanes 1 and 3). This stimulation requires PCNA, since in the absence of PCNA, RFC and RPA increased the DNA synthetic activity of hPol $\eta$  only ~2-fold (Fig. 3A, compare lanes 1 and 2). This weak enhancement could be attributed to RPA, since the addition of RPA alone also resulted in ~2-fold stimulation (Fig. 3, lane 8). This effect probably stems from a reduction in the nonspecific binding of hPol $\eta$  to single-stranded DNA by the presence of RPA. No stimulation of DNA synthesis occurred with PCNA or RFC alone (Fig. 3, lanes 6 and 7). As no significant stimulation of DNA synthesis occurs unless all three proteins are present (Fig. 3A, lanes 1 to 8), PCNA, RFC, and RPA cooperate to stimulate the activity of hPol $\eta$ . In contrast, the hPol $\eta$  A<sup>707-708</sup> and hPol $\eta$  (1-695) mutant proteins were greatly impaired in their ability to be stimulated by PCNA in the presence of RFC and RPA (Fig. 3A, compare lanes 9 and 10 or lanes 11 and 12).

**Effect of PCNA on the processivity of hPol $\eta$ .** Both yeast Pol $\eta$  and hPol $\eta$  are low-processivity enzymes, incorporating only a few nucleotides per DNA binding event (21, 38). A low processivity is desirable for this enzyme, in order to limit its activity to synthesizing only short stretches of DNA, thereby preventing the high mutation rates that would otherwise occur if this low-fidelity polymerase were to synthesize long tracts of DNA. However, the possibility existed that an increase in processivity was in fact responsible for stimulation of the activity of hPol $\eta$  by PCNA. To test if PCNA, together with RFC and RPA, increases the processivity of hPol $\eta$ , we used a circular single-stranded M13 template DNA primed singly with a 5' <sup>32</sup>P-labeled oligonucleotide primer. To ensure that we were observing deoxynucleotide incorporation resulting from a single DNA binding event, we monitored DNA synthesis in the presence of an excess of nonradiolabeled, sonicated herring

sperm DNA as a trap (Fig. 3B). The reactions were performed by first preincubating hPol $\eta$  in the absence (Fig. 3B, lanes 1 and 4) or in the presence (Fig. 3B, lanes 2 and 3) of PCNA, RFC, and RPA with the DNA substrate. All four dNTPs (Fig. 3B, lanes 1 and 2) or a mixture of excess herring sperm DNA and all four dNTPs (Fig. 3B, lanes 3 and 4) was then added to initiate the reaction. In the presence of the DNA trap, all hPol $\eta$  molecules that dissociate from the labeled DNA substrate will be bound by the excess of nonradiolabeled herring sperm DNA. The effectiveness of the trap was verified by first preincubating hPol $\eta$  with the DNA substrate together with the excess herring sperm DNA before the addition of nucleotides (Fig. 3B, lane 5). The lack of any DNA synthesis in this sample shows that the excess herring sperm DNA (about 100-fold) was sufficient to trap all hPol $\eta$  molecules. Despite the strong stimulation of hPol $\eta$  activity by PCNA, RFC, and RPA in the reactions containing no DNA trap (Fig. 3B, lane 2), in samples in which single-hit conditions were provided by excess herring sperm DNA, PCNA together with RFC and RPA stimulated the processivity of hPol $\eta$  only weakly; processivity remained low, at ~4 nucleotides per DNA binding event (Fig. 3B, compare lanes 3 and 4).

**Kinetic analysis of the DNA synthetic activity of hPol $\eta$  in the presence of PCNA.** To identify the mechanism by which PCNA stimulates the activity of hPol $\eta$ , we examined the steady-state kinetic parameters  $K_m$  and  $V_{max}$  for nucleotide insertion by hPol $\eta$  in the presence of PCNA, RFC, and RPA. Using a circular single-stranded M13 substrate DNA primed singly with a 5' <sup>32</sup>P-labeled oligonucleotide primer, we examined the kinetics of insertion of a single deoxynucleotide opposite an A residue in a standing-start reaction (Fig. 4A) or opposite a C residue in a running-start reaction (Fig. 4B) under steady-state conditions. From the kinetics of deoxynucleotide incorporation, the steady-state apparent  $K_m$  and  $V_{max}$  values for each deoxynucleotide were obtained from the curve fitted to the Michaelis-Menten equation. These  $K_m$  and  $V_{max}$

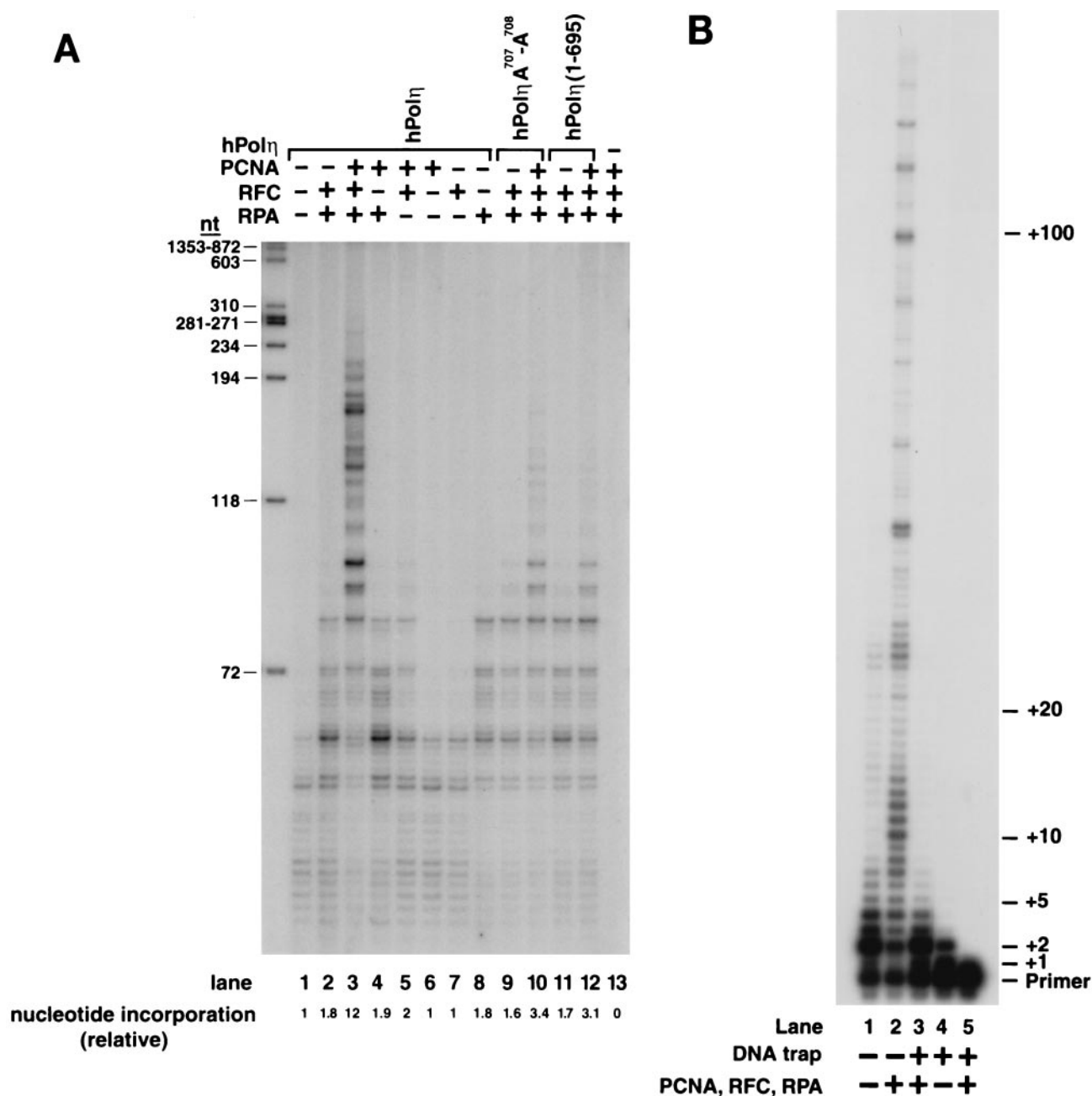


FIG. 3. Stimulation of DNA synthetic activity of hPol $\eta$  by PCNA. (A) DNA synthesis by the wild-type or PCNA binding site mutant hPol $\eta$  proteins in the presence or absence of PCNA, RFC, and RPA. The reaction mixtures contained either the wild type hPol $\eta$  protein (lanes 1 to 8) or the mutant hPol $\eta$  A<sup>707-708</sup> (lanes 9 and 10) or hPol $\eta$  (1-695) (lanes 11 and 12) proteins (10 ng each) along with singly primed M13 single-stranded DNA (25 ng), all four dNTPs (100  $\mu$ M each), [ $\alpha$ -<sup>32</sup>P]dATP, PCNA (100 ng), RFC (50 ng), or RPA (250 ng) or combinations of these proteins. No hPol $\eta$  was added in lane 13. The amount of DNA synthesis is indicated at the bottom as the relative nucleotide (nt) incorporation. *Hae*III-digested  $\phi$ X174 DNA labeled with polynucleotide kinase is shown on the left as a molecular size marker. (B) Processivity of hPol $\eta$  in the presence of PCNA, RFC, and RPA. hPol $\eta$  (10 ng) alone (lanes 1 and 4) or in the presence of PCNA (100 ng), RFC (50 ng), and RPA (250 ng) (lanes 2 and 3) was preincubated with a circular single-stranded M13 template DNA (50 ng) singly primed with a 5' <sup>32</sup>P-labeled oligonucleotide for 5 min at 37°C. Primer extension reactions were initiated by adding all four dNTPs (500  $\mu$ M each) (lanes 1 and 2) or all four dNTPs and excess sonicated herring sperm DNA (0.5 mg/ml) as a trap (lanes 3 and 4). After incubation for 10 min at 37°C, samples were quenched and run on a 10% polyacrylamide gel. To demonstrate the effectiveness of the trap, hPol $\eta$ , along with PCNA, RFC, and RPA, was preincubated with the trap DNA and the primer-template substrate before the addition of dNTPs (lane 5).

values and the efficiencies of nucleotide incorporation ( $V_{max}/K_m$ ) for hPol $\eta$  in the presence or absence of PCNA, RFC, and RPA are summarized in Table 2.

As indicated by the  $V_{max}/K_m$  values, hPol $\eta$  incorporates the

correct nucleotide about 15-fold more efficiently in the presence of PCNA, RFC, and RPA than in the absence of these proteins (Table 2). The incorporation of incorrect nucleotides is also stimulated by PCNA, RFC, and RPA (Fig. 4); however,

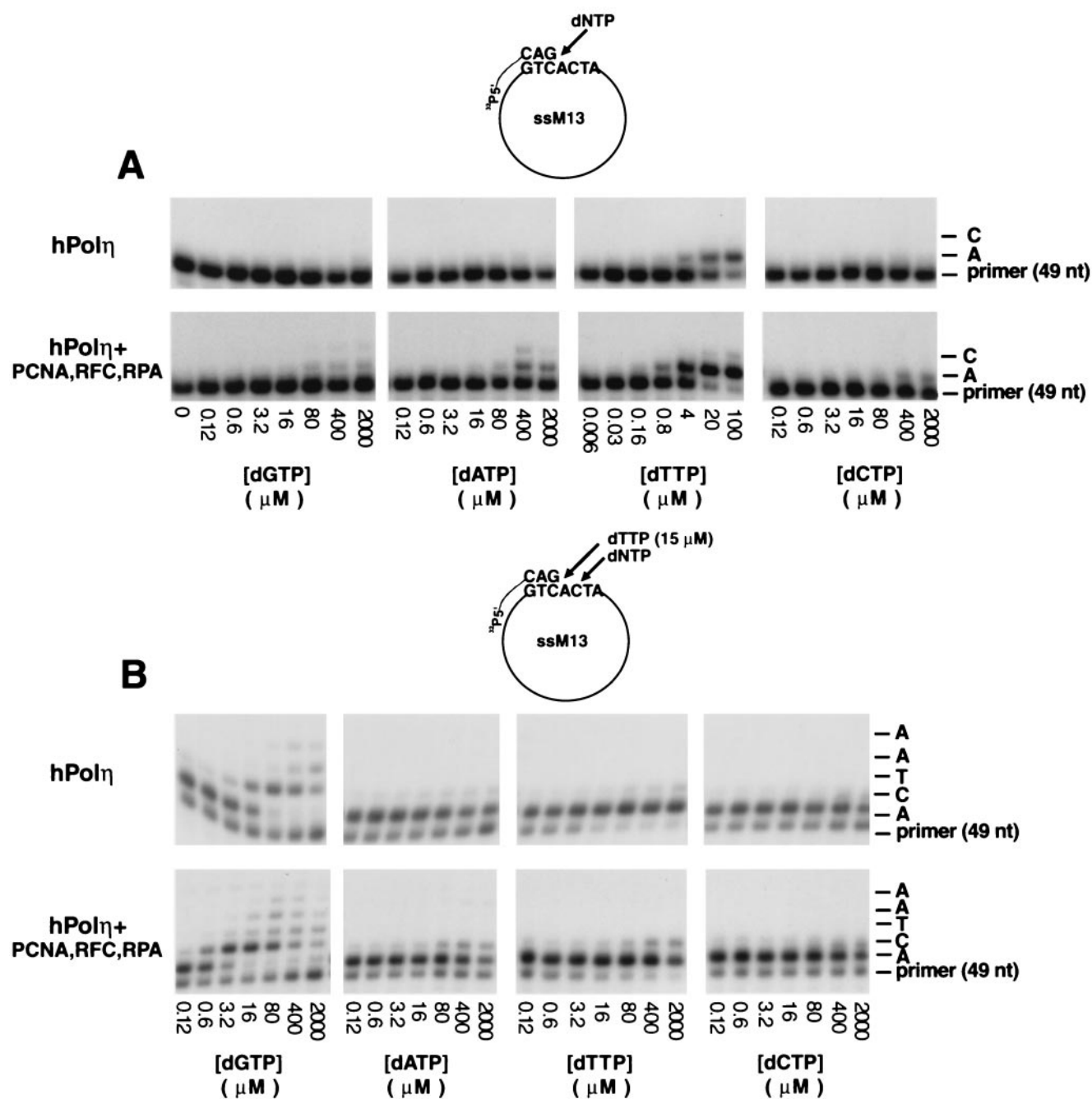


FIG. 4. PCNA stimulates deoxynucleotide incorporation by hPol $\eta$ . (A) Steady-state kinetics of deoxynucleotide incorporation opposite an A residue by hPol $\eta$  in the presence or absence of PCNA, RFC, and RPA in a standing-start reaction. A portion of the DNA substrate is shown at the top. Pol $\eta$  (10 ng) was incubated with a singly primed circular single-stranded M13 (ssM13) DNA substrate (25 ng) and increasing concentrations of a single deoxynucleotide in the absence or presence of PCNA (100 ng), RFC (50 ng), and RPA (250 ng). The nucleotide (nt) incorporation rate was plotted against the dNTP concentration, and the data were fit to the Michaelis-Menten equation describing a hyperbola. The apparent  $K_m$  and  $V_{max}$  values were obtained from the fit and used to calculate the efficiency of deoxynucleotide incorporation ( $V_{max}/K_m$ ). (B) Steady-state kinetics of deoxynucleotide incorporation opposite a template C residue by hPol $\eta$  in the presence or absence of PCNA, RFC, and RPA in a running-start reaction. Reactions were carried out as described for panel A, except that each reaction also included the addition of dTTP (15  $\mu$ M).

because of the low  $V_{max}$  values for the insertion of incorrect nucleotides in the absence of these proteins, we did not quantitate this enhancement. Importantly, PCNA, together with RFC and RPA, promotes nucleotide insertion by hPol $\eta$  primarily via an  $\sim$ 10- to 14-fold reduction in the apparent  $K_m$  for the nucleotide. In contrast, there was only a slight

increase in the  $V_{max}$  when PCNA, RFC, and RPA were present. As judged from the comparison of the  $V_{max}/K_m$  values for the incorporation of correct and incorrect nucleotides, the fidelity of nucleotide insertion of hPol $\eta$  in the presence of PCNA, RFC, and RPA remains low, ranging from  $8.5 \times 10^{-3}$  to  $2.7 \times 10^{-4}$ .

TABLE 2. Kinetic parameters for nucleotide insertion reactions catalyzed by hPol $\eta$ 

Reaction	Insertion	Site <sup>a</sup>	dNTP added	$K_m$ ( $\mu$ M) <sup>b</sup>	$V_{max}$ (%/min) <sup>b</sup>	$V_{max}/K_m$	$f_{inc}$ <sup>c</sup>
Standing start	Opposite an A by hPol $\eta$	5'----CAG ----GTCACT	dTTP	23.6 $\pm$ 1.3	5.6 $\pm$ 0.15	0.24	ND
			dGTP	70 $\pm$ 12	1.1 $\pm$ 0.05	0.016	5 $\times$ 10 <sup>-3</sup>
	Opposite an A by hPol $\eta$ + PCNA, RFC, and RPA	5'----CAG ----GTCACT	dATP	83 $\pm$ 28	2.3 $\pm$ 0.2	0.027	8.5 $\times$ 10 <sup>-3</sup>
			dTTP	2.7 $\pm$ 0.3	8.5 $\pm$ 0.3	3.15	1
			dCTP	102 $\pm$ 19	0.98 $\pm$ 0.08	0.0096	3 $\times$ 10 <sup>-3</sup>
Running start	Opposite a C by hPol $\eta$	5'----CAG ----GTCACT	dGTP	14.3 $\pm$ 1.5	6.6 $\pm$ 0.45	0.46	ND
			dGTP	1 $\pm$ 0.09	7.6 $\pm$ 0.43	7.6	1
	Opposite a C by hPol $\eta$ + PCNA, RFC, and RPA	5'----CAG ----GTCACT	dATP	82 $\pm$ 16	2.5 $\pm$ 0.41	0.03	3.9 $\times$ 10 <sup>-3</sup>
			dTTP	238 $\pm$ 51	2.8 $\pm$ 0.3	0.012	1.5 $\times$ 10 <sup>-3</sup>
			dCTP	380 $\pm$ 95	0.78 $\pm$ 0.45	0.002	2.7 $\times$ 10 <sup>-4</sup>

<sup>a</sup> Sequences represent a portion of the substrate, as also shown in Fig. 4. Boldfacing indicates the template base which directed nucleotide insertion.

<sup>b</sup> Values are reported as means and standard deviations.

<sup>c</sup>  $f_{inc}$ , frequency of nucleotide misincorporation. ND, not determined.

## DISCUSSION

Pol $\eta$  plays a key role in the error-free replication of UV-damaged DNA, and inactivation of Pol $\eta$  in humans results in the cancer-prone syndrome XP-V. However, the mechanism by which this important translesion synthesis DNA polymerase is recruited to the stalled replication machinery in humans has remained unclear so far. Here, we identify a PCNA binding motif in the C terminus of Pol $\eta$  and provide both in vivo and in vitro evidence for the physical interaction of hPol $\eta$  with PCNA. Mutations in the PCNA binding motif greatly reduce the affinity of hPol $\eta$  for PCNA, indicating a role for this motif in PCNA binding.

PCNA, together with RFC and RPA, stimulates the DNA synthetic activity of hPol $\eta$   $\sim$ 12-fold. However, this increase does not result from an increase in the processivity of the enzyme. We find that even in the presence of PCNA, RFC, and RPA, hPol $\eta$  processivity remains low, at three or four nucleotides per DNA binding event. The effect of PCNA on hPol $\eta$  processivity stands in sharp contrast to the large increase in processivity that occurs for Pol $\delta$  in the presence of PCNA, RFC, and RPA (30, 32). However, since Pol $\eta$  misincorporates nucleotides at a higher rate than Pol $\delta$ , any increase in Pol $\eta$  processivity would have conferred high mutagenicity.

Steady-state kinetic analyses showed that PCNA, RFC, and RPA increase the efficiency of hPol $\eta$  for inserting the correct nucleotide by  $\sim$ 15-fold, and this increase is achieved primarily by a reduction in the apparent  $K_m$  for the nucleotide. Even though the processivity of hPol $\eta$  is not significantly increased, the stimulation of its synthetic activity in the presence of PCNA, RFC, and RPA may be due to an increased affinity of the enzyme for the primer 3' end, as has been suggested for the stimulation in synthesis by *E. coli* PolV that occurs with RecA, single-stranded DNA binding protein, and the  $\beta, \gamma$ -complex (28). However, the possibility that PCNA, RFC, and RPA stimulate the activity of hPol $\eta$  by increasing the affinity of the enzyme for the incoming nucleotide cannot be ruled out.

*Saccharomyces cerevisiae* Pol $\eta$  and hPol $\eta$  resemble one another in their damage bypass ability, and they promote the error-free replication of UV-damaged DNA. Similar to the results reported here for hPol $\eta$ , evidence was recently pro-

vided for physical and functional interactions of yeast Pol $\eta$  (Pol $\eta$ ) with PCNA (12). Like that of hPol $\eta$ , the DNA synthetic activity of yeast Pol $\eta$  is stimulated  $\sim$ 15-fold in the presence of PCNA, RFC, and RPA; processivity, however, is not affected. Both yeast Pol $\eta$  and hPol $\eta$  are highly inefficient at inserting a nucleotide opposite an abasic site (14). However, yeast PCNA, together with yeast RFC and yeast RPA, greatly stimulates the ability of yeast Pol $\eta$  to insert a nucleotide opposite an AP site; by comparison to the  $\sim$ 14-fold increase in the efficiency of G insertion opposite the template C, the ability of yeast Pol $\eta$  to insert a G opposite an AP site is stimulated over 350-fold in the presence of these protein factors (12). Additionally, genetic studies with the yeast Pol $\eta$  mutant proteins unable to bind PCNA have shown that an interaction with PCNA is indispensable for the in vivo function of Pol $\eta$ . From these studies, we infer a crucial role for PCNA in the targeting of Pol $\eta$  to the replication machinery stalled at a lesion site and in promoting the efficient bypass of DNA lesions.

Pol $\delta$ , required for the replication of both the leading and the lagging strands, stalls at DNA lesion sites, such as cyclobutane pyrimidine dimers. While an interaction with PCNA would promote the targeting of Pol $\eta$  to the replication machinery stalled at a lesion site, the question remains as to how Pol $\eta$  displaces stalled Pol $\delta$  and gains access to the template-primer junction. Studies of human DNA replication have revealed that the Pol $\alpha$ -to-Pol $\delta$  switch is coordinated via competition for RPA (41). First, Pol $\alpha$  binds RPA for firm attachment to the primed site. After Pol $\alpha$  has synthesized the primer, RFC is able to bind RPA at the primed template junction and competes with Pol $\alpha$  for RPA, resulting in the release of Pol $\alpha$  from DNA. RFC then loads PCNA onto DNA. Next, Pol $\delta$  binds both PCNA and RPA and competes with RFC for these two proteins. This process results in the displacement of RFC from the 3' terminus and in the binding of Pol $\delta$  to the 3' terminus. RFC, however, remains bound to DNA via its interaction with RPA. The Pol $\delta$ -to-Pol $\eta$  switch differs from the Pol $\alpha$ -to-Pol $\delta$  switch in that whereas both Pol $\delta$  and Pol $\eta$  bind PCNA, Pol $\alpha$  does not. The Pol $\delta$ -to-Pol $\eta$  switch could occur in any of the following ways. First, Pol $\eta$  may compete with Pol $\delta$  for the 3' terminus opposite a lesion site, perhaps because Pol $\eta$  binds

such a terminus more tightly than does Pol $\delta$ , resulting in the release of Pol $\delta$  from the replication complex. Alternatively, the displacement of Pol $\delta$  may be a more active process, requiring the action of the Rad6-Rad18 complex, which is essential for the replication of damaged DNA (29) and which comprises ubiquitin-conjugating and DNA binding activities (1). Conjugation of ubiquitin to a stalled Pol $\delta$  subunit may destabilize the Pol $\delta$  interaction with PCNA as well as its binding to the 3' terminus. Finally, it is possible that Pol $\eta$  displaces Pol $\delta$  from the 3' terminus but that both polymerases remain in the replication ensemble via their binding to different monomers of the homotrimeric PCNA ring. This scenario raises the possibility of physical and functional interactions of Pol $\eta$  with Pol $\delta$  that may further affect the fidelity, processivity, or damage bypass ability of Pol $\eta$ .

#### ACKNOWLEDGMENTS

This work was supported by National Institutes of Health grants GM19261 and GM38559.

#### REFERENCES

- Bailey, V., S. Lauder, S. Prakash, and L. Prakash. 1997. Yeast DNA repair proteins Rad6 and Rad18 form a heterodimer that has ubiquitin conjugating, DNA binding, and ATP hydrolytic activities. *J. Biol. Chem.* **272**:23360–23365.
- Bambara, R. A., R. S. Murante, and L. A. Henricksen. 1997. Enzymes and reactions at the eukaryotic DNA replication fork. *J. Biol. Chem.* **272**:4647–4650.
- Bloom, L. B., X. Chen, D. K. Fygenon, J. Turner, M. O'Donnell, and M. F. Goodman. 1997. Fidelity of *Escherichia coli* DNA polymerase III holoenzyme The effects of  $\beta$ ,  $\gamma$  complex processivity proteins and  $\epsilon$  proofreading exonuclease on nucleotide misincorporation efficiencies. *J. Biol. Chem.* **272**:27919–27930.
- Brash, D. E. 1997. Sunlight and the onset of skin cancer. *Trends Genet.* **13**:410–414.
- Cai, J., E. Gibbs, F. Uhlmann, B. Phillips, N. Yano, M. O'Donnell, and J. Hurwitz. 1997. A complex consisting of human replication factor C, p40, p37, and p36 subunits is a DNA-dependent ATPase and an intermediate in the assembly of the holoenzyme. *J. Biol. Chem.* **272**:18974–18981.
- Canella, K. A., and M. M. Seidman. 2000. Mutation spectra in supF: approaches to elucidating sequence context effects. *Mutat. Res.* **450**:61–73.
- Creighton, S., L. B. Bloom, and M. F. Goodman. 1995. Gel fidelity assay measuring nucleotide misinsertion, exonucleolytic proofreading, and lesion bypass efficiencies. *Methods Enzymol.* **262**:232–256.
- Creighton, S., and M. F. Goodman. 1995. Gel kinetic analysis of DNA polymerase fidelity in the presence of proofreading using bacteriophage T4 DNA polymerase. *J. Biol. Chem.* **270**:4759–4774.
- Echols, H., and M. F. Goodman. 1991. Fidelity mechanisms in DNA replication. *Annu. Rev. Biochem.* **60**:477–511.
- Gibbs, E., Z. Kelman, J. M. Gulbis, M. O'Donnell, J. Kuriyan, P. M. Burgers, and J. Hurwitz. 1997. The influence of the proliferating cell nuclear antigen-interacting domain of p21 (CIP1) on DNA synthesis catalyzed by the human and *Saccharomyces cerevisiae* polymerase delta holoenzymes. *J. Biol. Chem.* **272**:2373–2381.
- Goodman, M. F., S. Creighton, L. B. Bloom, and J. Petruska. 1993. Biochemical basis of DNA replication fidelity. *Crit. Rev. Biochem. Mol. Biol.* **28**:83–126.
- Haracska, L., C. M. Kondratik, I. Unk, S. Prakash, and L. Prakash. 2001. Interaction with PCNA is essential for yeast DNA polymerase  $\eta$  function. *Mol. Cell* **8**:407–415.
- Haracska, L., S. Prakash, and L. Prakash. 2000. Replication past O<sup>6</sup>-methylguanine by yeast and human DNA polymerase  $\eta$ . *Mol. Cell. Biol.* **20**:8001–8007.
- Haracska, L., M. T. Washington, S. Prakash, and L. Prakash. 2001. Inefficient bypass of an abasic site by DNA polymerase  $\eta$ . *J. Biol. Chem.* **276**:6861–6866.
- Haracska, L., S.-L. Yu, R. E. Johnson, L. Prakash, and S. Prakash. 2000. Efficient and accurate replication in the presence of 7,8-dihydro-8-oxoguanine by DNA polymerase  $\eta$ . *Nat. Genet.* **25**:458–461.
- Johnson, R. E., L. Haracska, S. Prakash, and L. Prakash. 2001. Role of DNA polymerase  $\eta$  in the bypass of a (6-4) TT photoproduct. *Mol. Cell. Biol.* **21**:3558–3563.
- Johnson, R. E., C. M. Kondratik, S. Prakash, and L. Prakash. 1999. *hRAD30* mutations in the variant form of xeroderma pigmentosum. *Science* **285**:263–265.
- Johnson, R. E., S. Prakash, and L. Prakash. 1999. Efficient bypass of a thymine-thymine dimer by yeast DNA polymerase, Pol $\eta$ . *Science* **283**:1001–1004.
- Johnson, R. E., S. Prakash, and L. Prakash. 1999. Requirement of DNA polymerase activity of yeast Rad30 protein for its biological function. *J. Biol. Chem.* **274**:15975–15977.
- Johnson, R. E., M. T. Washington, S. Prakash, and L. Prakash. 1999. Bridging the gap: a family of novel DNA polymerases that replicate faulty DNA. *Proc. Natl. Acad. Sci. USA* **96**:12224–12226.
- Johnson, R. E., M. T. Washington, S. Prakash, and L. Prakash. 2000. Fidelity of human DNA polymerase  $\eta$ . *J. Biol. Chem.* **275**:7447–7450.
- Kelman, Z., and J. Hurwitz. 1998. Protein-PCNA interactions: a DNA-scanning mechanism? *Trends Biol. Sci.* **23**:236–238.
- Kelman, Z., N. Yao, and M. O'Donnell. 1995. *Escherichia coli* expression vectors containing a protein kinase recognition motif, His6-tag and hemagglutinin epitope. *Gene* **166**:177–178.
- Lee, S. H., T. Eki, and J. Hurwitz. 1989. Synthesis of DNA containing the simian virus 40 origin of replication by the combined action of DNA polymerases alpha and delta. *Proc. Natl. Acad. Sci. USA* **86**:7361–7365.
- Masutani, C., R. Kusumoto, A. Yamada, N. Dohmae, M. Yokoi, M. Yuasa, M. Araki, S. Iwai, K. Takio, and F. Hanaoka. 1999. The *XPV* (xeroderma pigmentosum variant) gene encodes human DNA polymerase  $\eta$ . *Nature* **399**:700–704.
- McDonald, J. P., A. S. Levine, and R. Woodgate. 1997. The *Saccharomyces cerevisiae RAD30* gene, a homologue of *Escherichia coli dinB* and *umuC*, is DNA damage inducible and functions in a novel error-free postreplication repair mechanism. *Genetics* **147**:1557–1568.
- Nakanishi, M., R. S. Robetorye, O. M. Pereira-Smith, and J. R. Smith. 1995. The C-terminal region of p21<sup>SD11/WAF1/CIP1</sup> is involved in proliferating cell nuclear antigen binding but does not appear to be required for growth inhibition. *J. Biol. Chem.* **270**:17060–17063.
- Pham, P., J. G. Bertram, M. O'Donnell, R. Woodgate, and M. F. Goodman. 2001. A model for SOS-lesion-targeted mutations in *Escherichia coli*. *Nature* **409**:366–370.
- Prakash, L. 1981. Characterization of postreplication repair in *Saccharomyces cerevisiae* and effects of *rad6*, *rad18*, *rev3* and *rad52* mutations. *Mol. Gen. Genet.* **184**:471–478.
- Prelich, G., M. Kostura, D. R. Marshak, M. B. Matthews, and B. Stillman. 1987. The cell-cycle regulated proliferating cell nuclear antigen is required for SV40 DNA replication *in vitro*. *Nature* **326**:471–475.
- Reynolds, N., E. Warbrick, P. A. Fantes, and S. A. MacNeill. 2000. Essential interaction between the fission yeast DNA polymerase  $\delta$  subunit Cdc27 and Pcn1 (PCNA) mediated through a C-terminal p21<sup>CIP1</sup>-like PCNA binding motif. *EMBO J.* **19**:1108–1118.
- Tan, C. K., C. Castillo, A. G. So, and K. M. Downey. 1986. An auxiliary protein for DNA polymerase  $\delta$  from fetal calf thymus. *J. Biol. Chem.* **261**:12310–12316.
- Thomas, D. C., J. D. Roberts, R. D. Sabatino, T. W. Myers, C.-K. Tan, K. M. Downey, A. G. So, R. A. Bambara, and T. A. Kunkel. 1991. Fidelity of mammalian DNA replication and replicative DNA polymerases. *Biochemistry* **30**:11751–11759.
- Wang, Y.-C., V. M. Maher, D. L. Mitchell, and J. J. McCormick. 1993. Evidence from mutation spectra that the UV hypermutability of xeroderma pigmentosum variant cells reflects abnormal, error-prone replication on a template containing photoproducts. *Mol. Cell. Biol.* **13**:4276–4283.
- Warbrick, E. 1998. PCNA binding through a conserved motif. *Bioessays* **20**:195–199.
- Warbrick, E., D. P. Lane, D. M. Glover, and L. S. Cox. 1995. A small peptide inhibitor of DNA replication defines the site of interaction between the cyclin-dependent kinase inhibitor p21WAF1 and proliferating cell nuclear antigen. *Curr. Biol.* **5**:275–282.
- Washington, M. T., R. E. Johnson, S. Prakash, and L. Prakash. 2000. Accuracy of thymine-thymine dimer bypass by *Saccharomyces cerevisiae* DNA polymerase  $\eta$ . *Proc. Natl. Acad. Sci. USA* **97**:3094–3099.
- Washington, M. T., R. E. Johnson, S. Prakash, and L. Prakash. 1999. Fidelity and processivity of *Saccharomyces cerevisiae* DNA polymerase  $\eta$ . *J. Biol. Chem.* **274**:36835–36838.
- Waters, H. L., S. Seetharam, M. M. Seidman, and K. H. Kraemer. 1993. Ultraviolet hypermutability of a shuttle vector propagated in xeroderma pigmentosum variant cells. *J. Invest. Dermatol.* **101**:744–748.
- Yu, S.-L., R. E. Johnson, S. Prakash, and L. Prakash. 2001. Requirement of DNA polymerase  $\eta$  for error-free bypass of UV-induced CC and TC photoproducts. *Mol. Cell. Biol.* **21**:185–188.
- Yuzhakov, A., Z. Kelman, J. Hurwitz, and M. O'Donnell. 1999. Multiple competition reactions for RPA order the assembly of the DNA polymerase  $\delta$  holoenzyme. *EMBO J.* **18**:6189–6199.